High-Resolution, Large-Area Fabrication of Compliant Electrodes via Laser Ablation for Robust, Stretchable Dielectric Elastomer Actuators and Sensors

Oluwaseun A. Araromi,* Samuel Rosset, and Herbert R. Shea*

Microsystems for Space Technologies Laboratory (LMTS), École Polytechnique Fédérale de Lausanne (EPFL), Rue de la Maladière 71B, Neuchâtel 2000, Switzerland

S *Supporting Information*

ABSTRACT: A key element in stretchable actuators, sensors, and systems based on elastomer materials are compliant electrodes. While there exist many methodologies for fabricating electrodes on dielectric elastomers, very few succeed in achieving high-resolution patterning over large areas. We present a novel approach for the production of mechanically robust, high-resolution compliant electrodes for stretchable silicone elastomer actuators and sensors. Cast, 2−50 μm thick poly(dimethylsiloxane) (PDMS)-carbon composite layers are patterned by laser ablation and subsequently bonded to a PDMS membrane by oxygen plasma activation.

The technique affords great design flexibility and high resolution and readily scales to large-area arrays of devices. We validate our methodology by producing arrays of actuators and sensors on up to A4-size substrates, reporting on microscale dielectric elastomer actuators (DEA) generating area strains of over 25%, and interdigitated capacitive touch sensors with high sensitivity yet insensitivity to substrate stretching. We demonstrate the ability to cofabricate highly integrated multifunctional transducers using the same process flow, showing the methodology's promise in realizing sophisticated and reliable complex stretchable devices with fine features over large areas.

KEYWORDS: *dielectric elastomer sensors, dielectric elastomer actuators, laser ablation, oxygen plasma-bonding, electroactive polymers*
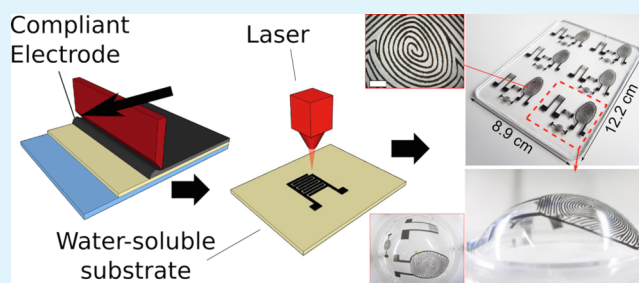
1. INTRODUCTION

In recent years the development of stretchable actuators and sensors based on the deformation of elastomers has received significant interest from researchers creating novel compliant and damage resilient systems, such as bioinspired sensor skins,[1] mechanically robust sensors,[2−4] high-strain electroactive actuators,[5,6] or foldable robotics.[7,8] We present a novel fabrication methodology for the production of large-area, high-resolution, and compliant electrodes for deformable and mechanically robust dielectric elastomer actuators (DEAs) and dielectric elastomer sensors (DESs). Our method is based on laser-patterned thin silicone-carbon composite layers bonded to silicone membranes using oxygen plasma activation. This approach combines the high-resolution, high-throughput, and large-area processing of laser patterning with the ability to use nearly any silicone elastomer membrane, while making use of water-soluble sacrificial layers to enable easy handling.

The realization of compliant electrodes is an important aspect in the development of DEAs and DESs. In DEAs, two compliant electrodes sandwich the elastomer membrane (usually a silicone or acrylic elastomer) and the application of a voltage bias (typically several kilovolts) across them causes thickness reduction and in-plane expansion of the membrane due to

electrostatic forces.[5] The resulting compressive stress (σ) through the thickness of the elastomer membrane is given by

$$\sigma = \varepsilon E^2 \tag{1}$$

where ε is the permittivity of the elastomer membrane and E is the applied electric field. The resulting in-plane strain (e) can be approximated by (for free boundary conditions):

$$e = \frac{\varepsilon E^2}{Y_{\mathrm{eff}}} \tag{2}$$

where Y_{eff} is the effective modulus of elasticity of the electrode—elastomer sandwich expressed by[9]

$$Y_{\mathrm{eff}} = \frac{Y_s t_s + 2 Y_e t_e}{t_s + 2 t_e} \tag{3}$$

where Y is the elastic modulus, t is the thickness, and the subscripts s and e refer to the silicone elastomer and electrodes, respectively. From eqs 2 and 3 it is clear that the electrodes must be as thin and compliant as possible, i.e., possessing preferably an

elastic modulus and thickness much lower than the elastomer, in order to maximize the strain produced in actuation.

In capacitive DESs, strain sensing is performed by detecting changes in the membrane capacitance,[10] and touch sensing is performed by detecting changes in the fringe field between parallel or coplanar electrodes.[3,11] Here the electrode compliance is required to enable the elastic properties of the elastomers to be fully exploited. Additionally electrodes for DEAs and DESs should remain conductive at high strains (>20%) and over a large number of cycles (>10^6), and maintaining their mechanical integrity during transduction or in the presence of externally applied mechanical deformations. Numerous electrode technologies for dielectric elastomer transducers have been investigated to date, as extensively reviewed in ref 9, including the following: deposited metallic thin layers,[16] implanting metallic particles in the elastomer surface,[17−19] carbon nanotube- or metallic nanoparticle-elastomer composites,[20,21] encapsulated liquid metal microchannels,[22−24] transparent hydrogels and ionogels,[25,26] and carbon (including graphite) loose powders, greases, or composites,[27−29] which are the most commonly used.

Methods based on metal films are attractive due to their high conductivities (<10 Ω sq^{-1}) but typically overstiffen the underlying elastomer, though unidirectional actuation has been achieved by microstructuring the elastomer membrane.[16] Ionic electrode methods (hydrogels and ionogels) are attractive due to their optical transparency but have yet to be demonstrated at high pattern resolution. Carbon-based methods have been used extensively by several researchers, for example in the development of actuators capable of large-area strains (>50%),[6,28,29] as these materials can be easily manipulated and have a relatively low stiffening impact on the elastomer membrane. Capacitive sensing has also been demonstrated using carbon-based electrodes.[10] Carbon powders dispersed in elastomer matrices in particular offer good mechanical robustness and the ability to tune the electrode conductivity.

Silicone elastomers are appealing materials for stretchable transducers, both for use as the elastomer dielectric or as the elastomer matrix in compliant electrodes. They are lightweight, can be processed easily using a variety of methods,[12,13] and are highly compliant, in some cases capable of being stretched >1000% without rupture. Moreover silicone elastomers are available in a wide range of elastic moduli, generally possess low viscous properties leading to fast electromechanical response times,[14,15] and can, as is the case for poly(dimethylsiloxane) (PDMS), be optically transparent.

Patterning polymers by laser ablation has been used in the past to fabricate microscale features,[30,31] and bonding of PDMS using oxygen plasma has been widely used in the microfluidics domain.[32,33] In this work we combine these processes together with thin film casting of compliant electrodes to create a novel fabrication method well suited to dielectric elastomer transducer fabrication. By decoupling the electrode patterning and bonding steps, our fabrication methodology enables easy scaling to large areas (>100 cm^2), for example for the production of device arrays (Figure 1A), while maintaining high-resolution features (Figure 1B,C). Once the electrode is bonded to the elastomer membrane, the water-soluble substrate is simply dissolved away in hot water (see Video S1 in the Supporting Information), providing an elegant electrode transfer solution. An additional advantage of our transfer method is the low mechanical stresses imposed on the elastomer membrane compared to other methods such as stamping or manual patterning; hence, our process can also be used with ultrathin elastomer films (<5 μm
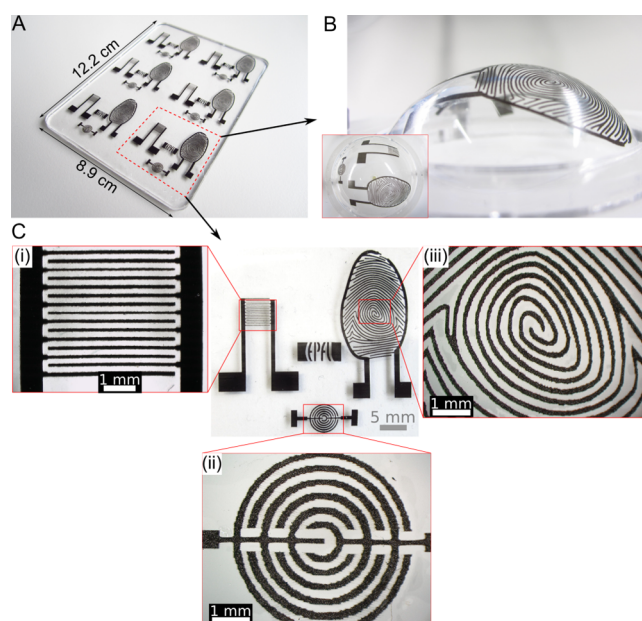

Figure 1. Interdigitated transducer geometries produced by laser ablation of cast carbon−silicone bonded to an elastomer: (A) Array of transducers, bonded to a thick PDMS substrate; (B) side view of transducers bonded to thin PDMS membrane and inflated, demonstrating their high deformability (inset, top view); (C) details of the different interdigitated transducer geometries (EPFL logo reprinted with permission from EPFL. Copyright 2015.), (i) rectangular, (ii) circular, and (iii) fingerprint shape. Resolution for these devices is simply set by the laser engraver used, not intrinsically by the method.

thickness) without causing rupture. The flexibility in the process facilitates short design iteration loops, allowing transducer designs to be fabricated, tested, and optimized quickly. Moreover our technique also facilitates the fabrication of highly integrated, multifunctional dielectric elastomer systems, i.e., capable of simultaneous sensing and actuation, on a single elastomer membrane with a single process flow, accelerating the development of sophisticated stretchable devices.

A description of our fabrication method is provided in the experimental section (section 2) along with details of the experiments conducted in this work. Characterization of the fabrication method in terms of adhesion, resistance versus stretch, and plasma-induced stiffening is provided in section 3.1. We then demonstrate the efficacy of our method in fabricating stretchable microscale actuators, capacitive touch sensors, and multifunctional devices capable of simultaneous actuation and sensing in sections 3.2 and 3.3.

2. EXPERIMENTAL SECTION

2.1. Generalized Fabrication Methodology. Our generalized fabrication methodology is outlined in Figure 2. The water-soluble sacrificial substrate is made by casting a poly(vinyl alcohol) (PVA) aqueous solution onto a poly(ethylene terephthalate) (PET) substrate (Figure 2A) to a width of 20 cm and length of 29 cm. The water in the PVA solution is allowed to evaporate for 12 h leaving behind a flexible film with a thickness of 40 μm. The composite electrode is made by ball mixing carbon black (Ketjenblack 300, AkzoNobel) with a soft PDMS (MED4901, NuSil; elastic modulus, approximately 0.1 MPa) at a 1:10 weight ratio. The electrode mixture is cast onto the PVA substrate to the desired thickness (Figure 2B) and subsequently cured in an oven (electrode planar dimensions, 15 cm by 26 cm; typical thickness, between 4 and 8 μm). The cured electrode and PVA substrate are peeled from the PET substrate and patterned by laser ablation using a CO_2 laser
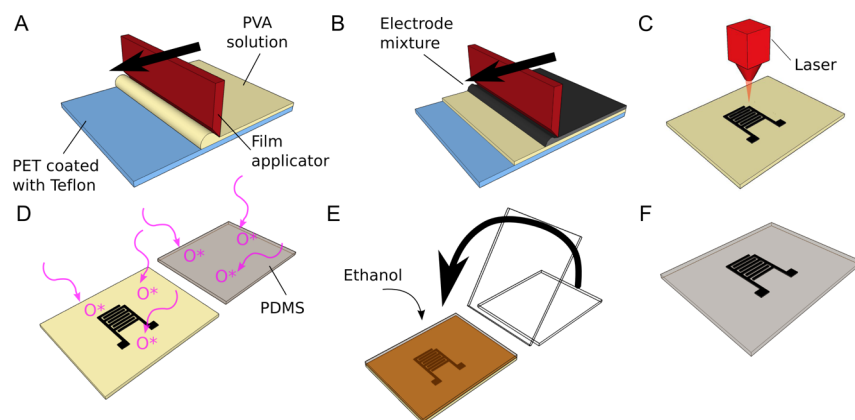
Figure 2. Schematic representation of the general fabrication procedure for compliant electrodes on thin silicone membranes: (A) PVA aqueous solution cast onto a PET film coated with PTFE (PVA planar dimensions, 20 cm × 29 cm); (B) casting of uncured electrode (planar dimensions, 15 cm × 26 cm); (C) cured electrode (typical thickness between 4 and 8 μm) and PVA substrate released from the PET film and the electrode patterned by laser ablation using a CO_2 laser engraver; (D) patterned electrode and separately prepared PDMS membrane treated in oxygen plasma; (E) treated surfaces of the patterned electrode and PDMS membrane placed in contact with each other to initiate bonding; (F) PVA substrate of the electrode dissolved in hot water until the PVA is completely removed (up to 10 min), leaving the electrode permanently bonded to the PDMS.

engraver (Speedy 300, Trotec; Figure 2C). The laser-patterned electrode and a separately prepared silicone membrane are treated in an oxygen plasma using a low-pressure plasma system (Zepto, Diener electronic) (Figure 2D) operating at 13.56 MHz, a chamber pressure between 0.2−0.3 mbar, and a power of 20 W. The treated surfaces are then placed in contact with each other to initiate bonding (Figure 2E); a small amount of ethanol is placed between the surfaces prior to placing them together in order to aid conformal contact. After 30 min the PVA substrate of the electrode is removed by dissolving in hot water (Figure 2F).

2.2. Selection of PDMS in Experiments. Sylgard 186 (Dow Corning; elastic modulus, approximately 1 MPa) was used as the dielectric in all DEAs experiments as it has been shown to perform well when used for DEAs.[7,8,14] Sylgard 186 membranes prestretched equi-biaxially by 1.33, with a final thickness of approximately 25 μm, were used in the plasma-induced stiffening and microactuator experiments. Membranes with a final thickness of 10 μm were used for the multifunction transducer experiments.

MED-4901 (NuSil) was used in the electrode mixture for all experiments, as the substrate in the capacitive sensor experiments and as encapsulating material in the multifunctional transducer experiments due to its low elastic modulus (approximately 0.1 MPa) and therefore low stiffening impact.

2.3. Resistance vs Strain Experiments. For the resistance vs strain measurements presented in Figure 3, the electrodes were bonded to a thick (100 μm) MED-4901 membrane to facilitate handling using an exposure time of 11 s. Resistance data were taken using a four-probe measurement to eliminate the effect of contact resistance. A Standa motorized stage (model 8MT175-150) driven at 0.5 mm s^{-1} was used to apply strains. After each measurement run, the strain was ramped down to 0% and the electrodes were allowed to recover over a period of at least 15 min before repeating the test.

2.4. Characterization of Plasma-Induced Stiffening. For the characterization of stiffening impact presented in Figure 4, only the region of the PDMS membrane covered by the electrode was exposed to the plasma in order to eliminate the mechanical coupling of the passive region (the region not covered by the electrode). Devices with stamped electrodes made using a TPM101 Teca print pad printing machine (further details on the stamping process are provided in the Supporting Information) were used for comparison. The elastomer membrane dimensions were 40 mm wide and 12.8 mm long (in the actuation direction); electrode dimensions were 30 mm wide and 4 mm long. PMMA elements of 1 mm thick, laser etched with image recognition markers, were bonded to the center of the membranes. The markers were used to track the actuator displacement, which was captured using a USB microscope. Image analysis was performed using a Labview script.
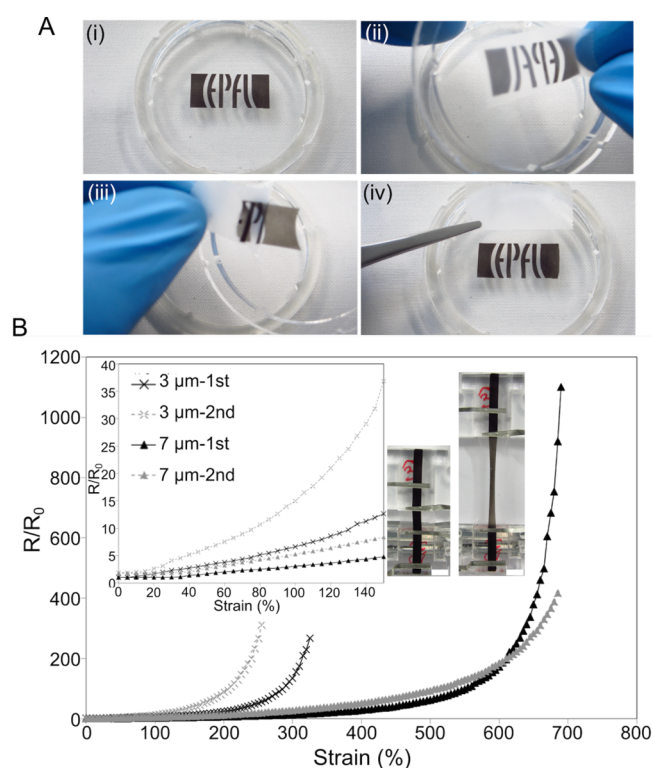

Figure 3. (A) Demonstration of the high adhesion of a patterned electrode to elastomer membrane, using the "Scotch-tape" test: 3 μm thick electrode patterned in the shape of the EPFL logo bonded to a 40 μm thick PDMS membrane, (i) electrode pattern before test (electrode bonded to back side of membrane), (ii) placing of adhesive tape on electrode surface, (iii) peeling off the tape, highly deforming the elastomer, and (iv) view of electrode and elastomer intact after tape removal. (B) Electrode resistance versus strain for 3 and 7 μm thick electrodes for two strain cycles up to 700%: values normalized to the initial resistance of each electrode, approximately 300 kΩ and 100 kΩ. Inset figures: zoom of strain region between 0 and 150% and images of the 7 μm thick electrode sample at 40% and 600% strain (scale bar = 5 mm). EPFL logo reprinted with permission from EPFL. Copyright 2015.
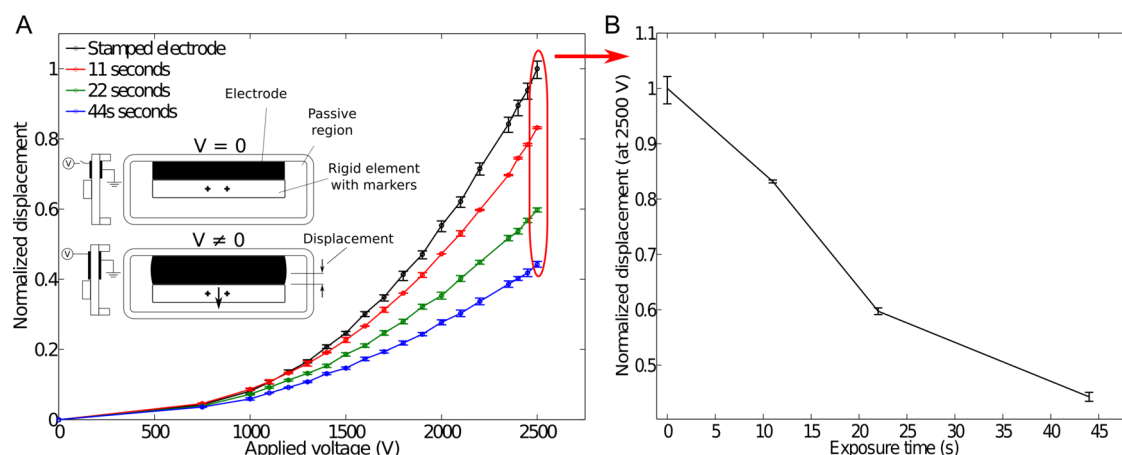
Figure 4. Actuation of DEAs showing the stiffening impact of oxygen plasma exposure: (A) actuator displacement for different plasma exposure times normalized by the displacement of the actuators with stamped (i.e., no plasma exposure) electrodes at 2.5 kV (error bars are maximum and minimum values of the samples used to make the average; inset shows actuator operating principle); (B) normalized actuator displacements from A at an applied voltage of 2.5 kV plotted as a function of plasma exposure time (datum at 0 s corresponds to stamped electrode). The 11 s time corresponds to the shortest time we used that allowed consistent high-strength bonding and retains 80% of maximum actuation strain compared to a plasma-free process.

2.5. Microactuators. For the microscale actuators presented in Figure 5, electrode lines of width approximately 100, 200, and 300 μm
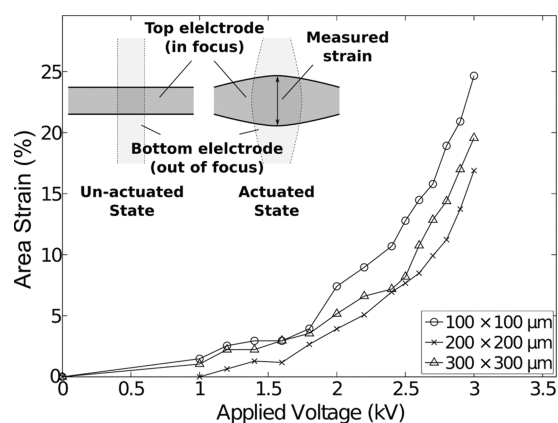

Figure 5. Cross-shaped DEA microactuators. Area strain vs drive voltage for microactuators of dimension 300 μm × 300 μm, 200 μm × 200 μm, and 100 μm × 100 μm made using 3 μm thick electrodes (plasma exposure time = 11 s for all devices).

were laser-ablated and plasma-bonded to the back and front sides of the PDMS membrane in a cross-pattern using a plasma exposure of 11 s. Input voltages between 0 and 3.0 kV were applied incrementally to the actuators using a high-voltage supply (EAP Controller, Auckland Biomimetics Laboratory) and held for 20 s. Pictures of the microactuators were taken at each voltage input using an optical microscope and the resulting strain measured using ImageJ software (National Institutes of Health). The area strain was determined using the width strain measured at the center of the top electrode, represented schematically in the inset of Figure 5 (assumed to be homogeneous over the active region and equal to the strain in the perpendicular direction.)

2.6. Interdigitated Capacitive Touch Sensor. The capacitive sensor presented in section 3.2 was fabricated using an electrode approximately 7 μm thick bonded to a 5 μm thick MED-4901 membrane using a plasma exposure time of 11 s. The device was subsequently encapsulated using a second, thicker MED-4901 membrane (20 μm), using the same plasma parameters, to protect it from contaminants and to facilitate handling. The resulting device is shown in Figure 6A. The sensor was characterized at 0% and 50% uniaxial strains in the direction perpendicular to the lines of the

interdigitated electrodes (Figure 6B inset). Change in impedance versus separation distance from grounded conductors and high-permittivity insulators encapsulated in a PDMS balloon were measured using an Agilent E4980A precision LCR (impedance−capacitance−resistance) meter at 1 kHz measurement frequency (Figure 6B,C). Details of the PDMS balloon fabrication and a schematic of the experimental setup are provided in the Supporting Information. A measurement was also taken using a PMMA probe (relative dielectric constant approximately equal to 2) at zero prestretch for comparison.

2.7. Multifunction Transducer. The multifunctional device presented in section 3.3 was made in two halves, the top half having one of the DEA electrodes, the sensor electrodes, and an encapsulation layer, and the other half having the bottom DEA electrode. The two halves were later bonded together back-to-back using oxygen plasma activation with an exposure time of 11 s (a schematic cross-section of the device is provided in Figure 7B). This design approach reduced the chance of device failure during actuation due to defects in the dielectric membranes. The electrodes for the device were 7 μm thick; the passivation layer for the sensor was a 10 μm thick MED-4901 membrane bonded by oxygen plasma using an exposure time of 11 s.

A Labview script was used to monitor the capacitance of the sensor and trigger cyclic actuation of the actuator at 3 Hz when the capacitance fell below a user specified threshold, i.e., when a touch input was detected (Figure 7C). The script was written such that the device operated in latching mode; i.e., the device continued actuating periodically until another touch input was detected. The sensor threshold to trigger actuation was set to a reactance of −325 MΩ, equivalent to 0.48 pF (assuming a series resistance−capacitance circuit model).

3. RESULTS AND DISCUSSION

3.1. Fabrication Characterization. With our laser system electrode line widths of less than 100 μm are achievable for electrodes of thickness ≤ 8 μm (Figure 1C). Significantly higher resolution (as low as 1 μm) should be achievable with laser technologies more optimized for high-resolution patterning, such as those using femtosecond lasers.[30,31]

The bonding created as a result of the oxygen plasma treatment produces transducers with excellent electrode adhesion, as qualitatively demonstrated in Figure 3A using a "Scotch-tape" test. This results in mechanically robust devices as resistant to damage as the underlying elastomer (see Video S2 of the Supporting Information). Moreover the plasma exposure was found not to be detrimental to electrode resistance. One
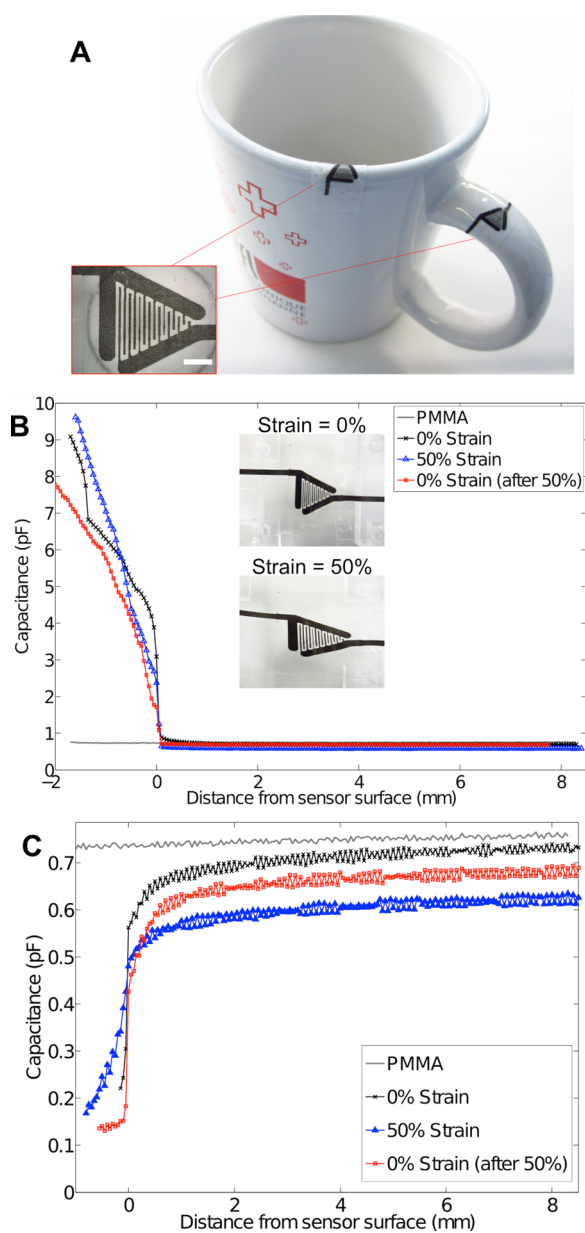
Figure 6. Interdigitated capacitive touch sensor with 300 μm pitch: (A) demonstration of sensor conformability to both high curvature and low curvature regions of a coffee mug (reprinted with permission from EPFL. Copyright 2015. Inset, closeup image of sensor (scale bar = 2 mm)); (B) sensor capacitance vs distance to a 13 mm diameter PDMS balloon filled with deionized water (high permittivity) approaching the sensor surface (inset, pictures of sensor at 0% and 50% strain); (C) sensor capacitance vs distance to a 13 mm diameter PDMS balloon filled with a grounded salt-water solution. In B and C zero on the horizontal axis corresponds to the point of first contact of the balloon with the sensor. Sensor response to a PMMA probe (low permittivity) provided for comparison.

Figure 7. Stretchable capacitive proximity sensor and dielectric elastomer actuator made on the same elastomer membrane. An external circuit is used to read the capacitance and apply a square wave voltage to the DEA when a finger is detected, causing the play logo to pulsate until another finger touch is detected. (A) Image of the device showing the actuator (shaded red) surrounding an interdigitated capacitive sensor (shaded green) and the passive area of the membrane (shaded blue). (B) Device cross-section schematic. (C) Response of sensor to finger touches directly on the sensor region. When the capacitance falls below 0.48 pF (corresponding to a valid touch input), a 2 kV periodic voltage input is applied to the actuator until a second touch input is detected. The sensor detects finger proximity, not strain: when the passive region of the membrane is touched, the device does not respond.

proposed mechanism for bonding is the reaction of oxygen radicals in the plasma with the methyl groups (-CH$_3$) of the PDMS chains, producing silanol (-OH) groups in their place, followed by condensation reaction to form covalent bonds once the treated surfaces are in contact.[32,34] After a period of approximately 30 min the PVA substrate is removed by dissolving in hot water. We are able to obtain good adhesion to a variety of commercially available PDMS membranes (listed
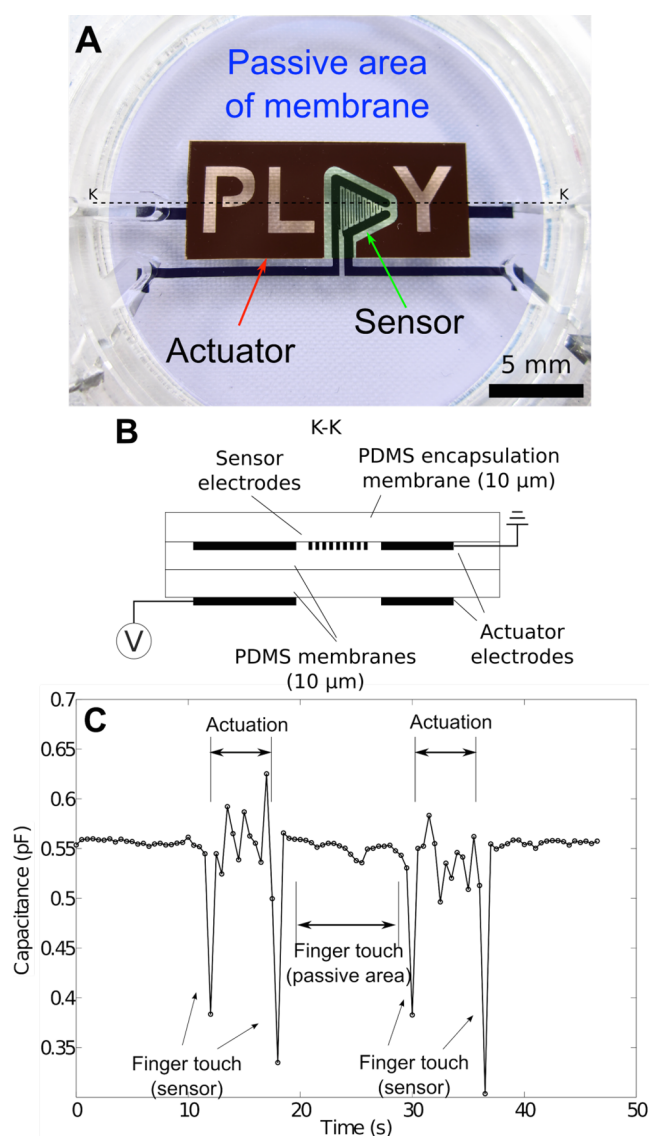
in the Supporting Information) using our approach, providing great flexibility in transducer design.

Casting the electrode enabled the electrode thickness—and therefore conductivity and stiffening impact—to be easily tailored according to the application requirements with reasonable thickness homogeneity (typically thickness variation under 1 μm). Moreover, our methodology is compatible with various carbon powder fillers and filler ratios, providing additional design flexibility. Figure 3B shows the resistance variation against uniaxial strain of 3 mm wide and 5 mm long electrode samples cast to a thickness of 3 and 7 μm (initial

resistances, approximately 300 kΩ and 100 kΩ, respectively). The results show that both electrodes remained conductive over strains of several hundred percent with the 7 μm thick electrode remaining conductive at strains of over 600%.

The maximum strain at which the electrodes lost conductivity was approximately double for the 7 μm thick electrode compared to the 3 μm electrode, implying a trade-off between the stiffening impact of the electrode on the PDMS membrane (an important consideration when fabricating DEAs) and the maximum strain for which the electrodes remain conductive. Note that for both electrode thicknesses the electrodes remained conductive after the strain was removed and reapplied, though the resistance at zero strain had increased in both cases and the maximum strain for which the electrode remained conductive had decreased for the 3 μm electrode. From a device perspective, this implies that a loss of conductivity resulting from extremely large externally applied deformations is nonfatal and that the conductivity will be recovered when the strain is released.

Exposure to oxygen plasma is known to progressively produce a silica-like layer on the surface of the treated PDMS.[35] This stiffens thin elastomer membranes and can thus reduce the strain produced by a DEA. We characterize this stiffening effect by measuring the actuation displacement generated by DEAs produced with different plasma exposure times using our technique. The actuator design is schematically shown in Figure 4A (inset); the device is optimized to produce in-plane, unidirectional displacement of a rigid element bonded to the prestretched membrane at its center, similar to the device reported in ref 36.

The electrodes were bonded using plasma exposure times of 11, 22, and 44 s, and the results compared with similar electrodes stamped directly on the PDMS membrane (i.e., no plasma exposure). The results also show a monotonic decrease in the normalized actuation displacement produced by the actuators in the applied voltage range for increasing plasma exposure time. The normalized displacement at a drive voltage of 2.5 kV vs plasma exposure time, Figure 4B, shows an approximately linear reduction in displacement with exposure time. Plasma exposure times should be minimized, to minimize stiffening of the elastomer, but must be long enough to achieve sufficient bonding for a given application (11 s for our system).

3.2. Transducers with Microscale Features. We use our approach to fabricate microsized DEAs, taking advantage of the high pattern resolution achievable by the laser ablation process. DEAs are seldom explored at the microscale though they have shown potential for the development of test assays for mechanotransduction studies of single or small biological cell populations[37] and for tunable diffraction gratings.[38] Micro-actuators of dimensions 300 μm × 300 μm, 200 μm × 200 μm, and 100 μm × 100 μm were fabricated by patterning orthogonal electrode lines on opposite sides of a PDMS membrane (Figure 5). The actuators were made using the same PDMS and prestretch as those used for the plasma-induced stiffening characterization in section 3.1. Area strains of up 25% were achievable within the voltage range of 0−3.0 kV, representing a safe operating range below the nominal breakdown field = 100 V/μm (from ref 39). These results show that functional microactuators can be produced using our technique, opening the door to further exploration of DEAs at the microscale.

We fabricated an interdigitated capacitive sensor with 300 μm pitch using our fabrication procedure (Figure 6A). The capacitance of the sensor changes in relation to the permittivity of the objects in its immediate vicinity, increasing when higher

permittivity insulators are close, or decreasing for grounded conductors (i.e., the human body).[3,11] Such sensors can be used for humidity sensing[40] and can also be used to detect touch or finger proximity. The interdigitated design is advantageous from a fabrication point of view in that the sensing electrodes are coplanar, enabling device fabrication on one membrane surface with a single bonding step. Moreover, the coplanarity of the electrodes makes the device inherently vastly less sensitive to mechanical deformations of the elastomer membrane compared to typical parallel plate capacitive designs. The response of our sensor as a function of the distance of a PDMS balloon filled with deionized water (high-permittivity insulator) and a grounded salt-water solution from the sensor surface is shown Figure 6 (experimental setup is shown in Figure S3 of the Supporting Information).

The results show an increase in the capacitance of at least 100% between the point of initial contact (point at which separation distance = 0 mm) and noncontact states for the deionized water experiment, and at least a 30% decrease for the grounded ionic solution at 0% strain. The sensor response increases further by several hundred percent compared to the baseline value as the deionized water balloon advances and covers more of the sensor area. The inverse effect can be seen with the grounded ionic solution balloon as it advances, with a capacitance reduction of almost 80% relative to the baseline value. These results indicate an increased sensitivity compared to stretchable parallel plate capacitive touch sensors of the same size scale[3,11]—the result of the interdigitated approach—further highlighting the utility of our high-resolution patterning capability.

When the sensor is stretched by 50%, the baseline capacitance value decreases by approximately 20%; however, the final values of capacitance are maintained with both the deionized water and grounded ionic solution. We draw the following conclusions from these results: (1) the sensor remains functional even when highly mechanically deformed, (2) the capacitance change relative to the baseline (unstretched) value is maintained even when stretched up to 50% uniaxially, and (3) even at these strains the change in baseline capacitance is lower than the change brought about by the stimuli, providing insensitivity to cross-talk, which is an issue for stretchable parallel plate capacitive sensors.[4] This therefore greatly increases the potential for achieving compact and high-resolution stretchable touch sensor arrays. Additionally, for applications requiring a high degree of conformability to an object (such as sensor skins) this property allows the sensors to be deformed and stretched around objects of various shapes and curvatures (Figure 6A) while remaining functional. Once the 50% strain was released the baseline capacitance decreased slightly (probably due to viscoelastic creep) as seen in Figure 6C. However, the sensor remained fully functional, with a sensitivity close to its initial value.

3.3. Multifunctional Transducers. We further highlight the versatility of our fabrication method by producing a multifunctional demonstrator device capable of both touch sensing and actuation simultaneously (Figure 7). The touch sensor is an interdigitated capacitive sensor similar to that presented in section 3.2, and the actuator (pulsing play logo) follows the DEA working principle explained in section 1. The multifunctional device has a highly integrated design with the sensor located in the middle of the actuator region, resulting in a compact device (Figure 7A). The actuator ground electrode and capacitive sensor were patterned on the same electrode substrate and

bonded to a prestretched elastomer membrane with a single plasma-bonding step.

Figure 7C shows the sensor response during device operation in which a user's touch input initiates actuation (see Video S3 of the Supporting Information). During actuation, small variations in the capacitance could be observed, related to the high electric fields used for actuation. However, these variations were small compared to the touch input enabling subsequent touch inputs to be clearly discriminated. Touch inputs were also applied to the passive areas of the device membrane (Figure 7C), the device proved to be insensitive to these inputs, highlighting once again the sensor's impressive resilience to mechanical perturbations.

4. CONCLUSION

A novel fabrication methodology for high-resolution patterning of compliant electrodes for stretchable dielectric elastomer actuators and sensors was presented. The approach uses cast PDMS-carbon electrodes patterned by laser ablation and achieves robust permanent bonding to a silicone elastomer membrane by oxygen plasma activation. We demonstrate the flexibility of our methodology in fabricating a variety of transducer designs with sub-200 μm feature sizes over large areas (over 100 cm^2). The process readily scales to much larger areas. The stiffening effect of the plasma exposure was characterized and shown to increase monotonically with exposure time. Excellent adhesion between the electrode and elastomer membranes can be achieved even with low (11 s) exposure times. Both functional microactuators and interdigitated capacitive sensors have been demonstrated with our technique. The capacitive sensor in particular showed excellent performance, maintaining high sensitivity even when stretched up to 50%. Conversely the baseline change in capacitance was comparatively small even at these strains, providing insensitivity to mechanical perturbations and cross-talk, and opening the potential to more compact stretchable touch sensor arrays. These results validate our technique as being a reliable and flexible platform from which to further explore microscale stretchable DEAs and DESs. We combined sensing and actuation in one multifunctional device demonstrator fabricated with the same process flow, combining high-resolution robust electrodes with large-area processing, showing the potential of our technique to produce sophisticated and highly integrated multifunction stretchable devices.

ASSOCIATED CONTENT

Ⓢ Supporting Information

The Supporting Information is available free of charge on the ACS Publications website at DOI: 10.1021/acsami.5b04975.

> Additional figures showing determination of laser ablation parameters, schematic of pad printing process, experimental setup schematic and photograph, and design and experimental setup for multifunctional device and and text giving experimental details (PDF).
>
> Three movies demonstrating fabriction results (QT).

AUTHOR INFORMATION

Corresponding Authors
*(O.A.A.) E-mail: seun.araromi@epfl.ch.
*(H.R.S.) E-mail: herbert.shea@epfl.ch.

Notes
The authors declare no competing financial interest.

REFERENCES

(1) Bauer, S.; Bauer-Gogonea, S.; Graz, I.; Kaltenbrunner, M.; Keplinger, C.; Schwödiauer, R. 25th Anniversary Article: A Soft Future: From Robots and Sensor Skin to Energy Harvesters. *Adv. Mater.* **2014**, *26*, 149−161.

(2) Vandeparre, H.; Watson, D.; Lacour, S. P. Extremely Robust and Conformable Capacitive Pressure Sensors Based on Flexible Polyurethane Foams and Stretchable Metallization. *Appl. Phys. Lett.* **2013**, *103*, 204103.

(3) Cotton, D. P. J.; Graz, I. M.; Lacour, S. P. A Multifunctional Capacitive Sensor for Stretchable Electronic Skins. *IEEE Sens. J.* **2009**, *9*, 2008−2009.

(4) Yao, S.; Zhu, Y. Nanomaterial-Enabled Stretchable Conductors: Strategies, Materials and Devices. *Adv. Mater.* **2015**, *27*, 1480−1511.

(5) Pelrine, R.; Kornbluh, R.; Pei, Q.; Joseph, J. High-Speed Electrically Actuated Elastomers with Strain Greater than 100%. *Science* **2000**, *287*, 836−839.

(6) Akbari, S.; Rosset, S.; Shea, H. R. Improved Electromechanical Behavior in Castable Dielectric Elastomer Actuators. *Appl. Phys. Lett.* **2013**, *102*, 071906.

(7) Araromi, O. A.; Gavrilovich, I.; Shintake, J.; Rosset, S.; Richard, M.; Gass, V.; Shea, H. R. Rollable Multisegment Dielectric Elastomer Minimum Energy Structures for a Deployable Microsatellite Gripper. *IEEE Trans. Mech.* **2014**, *20*, 438−446.

(8) Shintake, J.; Rosset, S.; Schubert, B. E.; Floreano, D.; Shea, H. R. A Foldable Antagonistic Actuator. *IEEE/ASME Trans. Mechatronics* **2014**, *PP*, 1−12.

(9) Rosset, S.; Shea, H. R. Flexible and Stretchable Electrodes for Dielectric Elastomer Actuators. *Appl. Phys. A: Mater. Sci. Process.* **2013**, *110*, 281−307.

(10) Gisby, T. A.; O'Brien, B. M.; Anderson, I. A. Self Sensing Feedback for Dielectric Elastomer Actuators. *Appl. Phys. Lett.* **2013**, *102*, 193703.

(11) Hu, W.; Niu, X.; Zhao, R.; Pei, Q. Elastomeric Transparent Capacitive Sensors Based on an Interpenetrating Composite of Silver Nanowires and Polyurethane. *Appl. Phys. Lett.* **2013**, *102*, 083303.

(12) Lotz, P.; Matysek, M.; Schlaak, H. F. Fabrication and Application of Miniaturized Dielectric Elastomer Stack Actuators. *IEEE Trans. Mech.* **2011**, *16*, 58−66.

(13) Maffli, L.; Rosset, S.; Shea, H. R. Zipping Dielectric Elastomer Actuators: Characterization, Design and Modeling. *Smart Mater. Struct.* **2013**, *22*, 104013.

(14) Maffli, L.; Rosset, S.; Ghilardi, M.; Carpi, F.; Shea, H. Ultrafast All-Polymer Electrically Tunable Silicone Lenses. *Adv. Funct. Mater.* **2015**, *25*, 1656−1665.

(15) Michel, S.; Zhang, X. Q.; Wissler, M.; Löwe, C.; Kovacs, G. A Comparison between Silicone and Acrylic Elastomers as Dielectric Materials in Electroactive Polymer Actuators. *Polym. Int.* **2010**, *59*, 391−399.

(16) Benslimane, M.; Gravesen, P.; Sommer-Larsen, P. Mechanical Properties of Dielectric Elastomer Actuators with Smart Metallic Compliant Electrodes. In *Electroactive Polymer Actuators and Devices (EAPAD) 2002*, Proceedings of SPIE, Vol. *4695*, San Diego, CA, USA, Mar. 17−21, 2002; Bar-Cohen, Y., Ed.; SPIE: Bellingham, WA, USA, 2011; p 150, DOI: 10.1117/12.475160.

(17) Niklaus, M.; Shea, H. R. Electrical Conductivity and Young's Modulus of Flexible Nanocomposites Made by Metal-Ion Implantation of Polydimethylsiloxane: The Relationship between Nanostructure and Macroscopic Properties. *Acta Mater.* **2011**, *59*, 830−840.

(18) Rosset, S.; Niklaus, M.; Dubois, P.; Shea, H. R. Metal Ion Implantation for the Fabrication of Stretchable Electrodes on Elastomers. *Adv. Funct. Mater.* **2009**, *19*, 470−478.

(19) Corbelli, G.; Ghisleri, C.; Marelli, M.; Milani, P.; Ravagnan, L. Highly Deformable Nanostructured Elastomeric Electrodes with Improving Conductivity upon Cyclical Stretching. *Adv. Mater.* **2011**, *23*, 4504−4508.

(20) Yun, S.; Niu, X.; Yu, Z.; Hu, W.; Brochu, P.; Pei, Q. Compliant Silver Nanowire-Polymer Composite Electrodes for Bistable Large Strain Actuation. *Adv. Mater.* **2012**, *24*, 1321−1327.

(21) Yuan, W.; Hu, L. B.; Yu, Z. B.; Lam, T.; Biggs, J.; Ha, S. M.; Xi, D. J.; Chen, B.; Senesky, M. K.; Grüner, G.; Pei, Q. Fault-Tolerant Dielectric Elastomer Actuators Using Single-Walled Carbon Nanotube Electrodes. *Adv. Mater.* **2008**, *20*, 621−625.

(22) Kubo, M.; Li, X.; Kim, C.; Hashimoto, M.; Wiley, B. J.; Ham, D.; Whitesides, G. M. Stretchable Microfluidic Radiofrequency Antennas. *Adv. Mater.* **2010**, *22*, 2749−2752.

(23) Tabatabai, A.; Fassler, A.; Usiak, C.; Majidi, C. Liquid-Phase Gallium-Indium Alloy Electronics with Microcontact Printing. *Langmuir* **2013**, *29*, 6194−6200.

(24) Park, M.; Park, J.; Jeong, U. Design of Conductive Composite Elastomers for Stretchable Electronics. *Nano Today* **2014**, *9*, 244−260.

(25) Keplinger, C.; Sun, J.-Y.; Foo, C. C.; Rothemund, P.; Whitesides, G. M.; Suo, Z. Stretchable, Transparent, Ionic Conductors. *Science* **2013**, *341*, 984−987.

(26) Chen, B.; Lu, J. J.; Yang, C. H.; Yang, J. H.; Zhou, J.; Chen, Y. M.; Suo, Z. Highly Stretchable and Transparent Ionogels as Nonvolatile Conductors for Dielectric Elastomer Transducers. *ACS Appl. Mater. Interfaces* **2014**, *6*, 7840−7845.

(27) Michel, S.; Chu, B. T. T.; Grimm, S.; Nüesch, F. A.; Borgschulte, A.; Opris, D. M. Self-Healing Electrodes for Dielectric Elastomer Actuators. *J. Mater. Chem.* **2012**, *22*, 20736.

(28) Huang, J.; Lu, T.; Zhu, J.; Clarke, D. R.; Suo, Z. Large, Uni-Directional Actuation in Dielectric Elastomers Achieved by Fiber Stiffening. *Appl. Phys. Lett.* **2012**, *100*, 211901.

(29) Keplinger, C.; Li, T.; Baumgartner, R.; Suo, Z.; Bauer, S. Harnessing Snap-through Instability in Soft Dielectrics to Achieve Giant Voltage-Triggered Deformation. *Soft Matter* **2012**, *8*, 285−288.

(30) Wolfe, D. B.; Ashcom, J. B.; Hwang, J. C.; Schaffer, C. B.; Mazur, E.; Whitesides, G. M. Customization of Poly(dimethylsiloxane) Stamps by Micromachining Using a Femtosecond-Pulsed Laser. *Adv. Mater.* **2003**, *15*, 62−65.

(31) Buitinga, M.; Truckenmüller, R.; Engelse, M. A.; Moroni, L.; Ten Hoopen, H. W. M.; van Blitterswijk, C. A.; de Koning, E. J. P.; van Apeldoorn, A. A.; Karperien, M. Microwell Scaffolds for the Extrahepatic Transplantation of Islets of Langerhans. *PLoS One* **2013**, *8*, e64772.

(32) Bhattacharya, S.; Datta, a.; Berg, J. M.; Gangopadhyay, S. Studies on Surface Wettability of Poly(dimethyl) Siloxane (PDMS) and Glass under Oxygen-Plasma Treatment and Correlation with Bond Strength. *J. Microelectromech. Syst.* **2005**, *14*, 590−597.

(33) Jo, B.-H.; Van Lerberghe, L. M.; Motsegood, K. M.; Beebe, D. J. Three-Dimensional Micro-Channel Fabrication in Polydimethylsiloxane (PDMS) Elastomer. *J. Microelectromech. Syst.* **2000**, *9*, 76−81.

(34) Mcdonald, J. C.; Duffy, D. C.; Anderson, J. R.; Chiu, D. T.; et al. Fabrication of Microfluidic Systems in Poly (dimethylsiloxane). *Electrophoresis* **2000**, *21*, 27−40 (Review).

(35) Kim, J.; et al. Hydrophobic Recovery of Polydimethylsiloxane Elastomer Exposed to Partial Electrical Discharge. *J. Colloid Interface Sci.* **2000**, *226*, 231−236.

(36) Rosset, S.; Araromi, O. A.; Shea, H. R. Maximizing the Displacement of Compact Planar Dielectric Elastomer Actuators. *Extrem. Mech. Lett.* **2015**, *3*, 72−81.

(37) Akbari, S.; Shea, H. R. An Array of $100\mu m \times 100\mu m$ Dielectric Elastomer Actuators with 80% Strain for Tissue Engineering Applications. *Sens. Actuators, A* **2012**, *186*, 236−241.

(38) Aschwanden, M.; Stemmer, A. Low Voltage, Highly Tunable Diffraction Grating Based on Dielectric Elastomer Actuators. In *Electroactive Polymer Actuators and Devices (EAPAD) 2007*, Proceedings of SPIE, Vol. *6524*, San Diego, CA, USA, Mar. 19−22, 2007; Bar-Cohen, Y., Ed.; SPIE: Bellingham, WA, USA, 2007; p 65241N, DOI: 10.1117/12.713325.

(39) Araromi, S.; Romano, P.; Rosset, S.; Perruisseau-Carrier, J.; Shea, H. A Tunable Millimeter-Wave Phase Shifter Driven by Dielectric Elastomer Actuators. In *Electroactive Polymer Actuators and Devices (EAPAD) 2014*, Proceedings of SPIE, Vol. *9056*, San Diego, CA, USA, Mar. 10−13, 2014; Bar-Cohen, Y., Ed.; SPIE: Bellingham, WA, USA, 2014; 90562M, DOI: 10.1117/12.2044589.

(40) Molina-Lopez, F.; Briand, D.; de Rooij, N. F. All Additive Inkjet Printed Humidity Sensors on Plastic Substrate. *Sens. Actuators, B* **2012**, *166−167*, 212−222.